

## MEASUREMENTS OF ATMOSPHERIC X AND GAMMA RAYS-BALLOON EXPERIMENTS AT SUBANTARTIC REGION

U.B. JAYANTHI, R.V. CORRÊA and F.G. BLANCO

*Instituto de Pesquisas Espaciais – INPE  
C.P. 515, 12201 – São José dos Campos, SP, Brazil*

The results of the stratospheric balloon experiments conducted to measure the atmospheric X and gamma rays are presented. These experiments, conducted at Commandante Ferraz base in sub antarctic region have provided the spectrum of ground radioactivity in gamma rays (0,2 to 2,9 MeV) and atmospheric X-ray spectra at different altitudes. We particularly choose to discuss the observed ceiling spectrum of X-rays in the 28 to 180 KeV region observed at  $7.0\text{g}\cdot\text{cm}^{-2}$ . We have utilized the data of other experiments with different telescope geometries, to evaluate the build-up effects due to cosmic ray secondaries in atmosphere. This behaviour previously studied for atmospheric gamma rays, permitted us to compare the ratio of up/down flux to explain the observed atmospheric X-ray spectrum.

Apresentam-se os resultados de dois vôos de experimentos a bordo de balões estratosféricos para medir raios X e gama atmosféricos. Estes experimentos, realizados na base Comandante Ferraz na região sub-Antártica, forneceram o espectro da radioatividade do solo em raios gama (0,2 a 2,9 MeV) e os espectros atmosféricos em raios X em diferentes alturas. Particularmente, discute-se o espectro de raios X observado no teto, em  $7\text{g}\cdot\text{cm}^{-2}$ , na região de energia entre 28 e 180 KeV. Utilizamos os dados de outros grupos com geometria de telescópios diferentes, para estudar os efeitos da multiplicação de raios cósmicos secundários na atmosfera. Este estudo, feito previamente para raios gama atmosféricos, permitiu-nos comparar a razão "up/down" dos fluxos para explicar o espectro de raios X atmosféricos observado.

### INTRODUCTION

The atmospheric X and gamma ray events observed by detectors at stratospheric balloon altitudes are the products of complex electromagnetic interactions of cosmic ray secondaries with the constituents of the atmosphere. The complex nature of these interactions prevent a direct translation of the observed spectrum to specific photon-particle or photon-photon interactions. As such the atmospheric background has been quantified in gamma ray energy range in terms of source function (Ling, 1975). To evaluate this source function, dependent on energy, atmospheric depth and geographical position, semiempirical models have been postulated from the observed fluxes.

The observed X and gamma ray atmospheric background has been verified in experiments to have latitudinal dependence, consistent with the increase in cosmic ray flux at higher latitudes (Jayanthi et al. 1982). In addition to this steady cosmic ray produced component, at higher latitudes near around auroral regions and in South Atlantic Anomaly region temporal flux increases by large factors have been observed (Anderson, 1960; Tepley & Wentworth, 1962; Martin et al., 1973; Pinto, Jr. & Gonzalez, 1986).

The Commandante Ferraz base at Antarctic is situated at high latitude to observe large fluxes of atmospheric

X and gamma ray background and perhaps temporal events due to auroral bursts, pulsations and precipitation events in the flight trajectory of the balloon as this region borders both South Atlantic Anomaly and southern auroral zone (Seward, 1973). We have conducted two balloon experiments one with X-ray detector and another with gamma ray detector in this region to observe atmospheric background. We describe the experiments and the results obtained in these balloon experiments.

### EXPERIMENTS AND FLIGHT DETAILS

The telescope for X-ray observations employed a 1,27cm thick NaI(Tl) scintillation detector (dia: 7.62cm) with an aluminum entrance window of 81 micron thick, to allow X-ray detection above 25 keV. The detector's view angle for X-rays incident in the forward direction was defined by a passive graded shield consisting of cylindrical sheets of 2mm thick brass and 1mm thick lead materials. This shield, which extends to enclose the sides of the X-ray crystal permitted FWHM  $\sim 24,5^\circ$  and  $\sim 30^\circ$  at 40 keV and 122 keV respectively. An active anti-coincidence detector of 1.25cm thick NE 102 plastic scintillator, in the shape of cylindrical well, enclosed the X-ray detector assembly and the graded shield to prevent charge

particle interactions which may mimic X-rays in the NaI (T1).

The X-ray detector events not in coincidence with the particle shield detector, were utilized for energy and temporal analysis. A discrete, linear pulse height analyser (PHA) sorted an equivalent of 28.5 to 185 keV X-ray events into 31 bins. The same events in parallel, were analysed by a time analyser with a time resolution of  $\sim 64$  msec. Data from PHA, time analyser, total count rate and anticoincidence count rate were accumulated for 2 minutes of duration in the payload for transmission by FM/FM telemetry along with pressure data.

The gamma ray telescope was an omnidirectional and employed a 7.62 X 7.62cm cylindrical NaI(T1) detector monitoring gamma ray events. An NE 102 plastic scintillator of  $\sim 1.25$ cm thick, in the shape of well, covered the NaI(T1) detector assembly on the bottom and sides to reject particle events in the gamma ray detector. A 256 channel analyser monitored the gamma events in the 0.2 to 5.3 MeV energy domain. The PHA analysed gamma ray events were accumulated for duration  $\sim 1$  minute before entering the FM/FM telemetry for transmission along with the total count rate, anti-coincidence rate and pressure sensor data.

Pre-flight calibrations have been extensively conducted on both X-ray and gamma ray payloads for the detector response, linearity and resolution of the detector and electronics, angular response of the telescope and anti-coincidence rejection efficiency etc., with various radioactive sources  $\text{Am}^{241}$ ,  $\text{Eu}^{152}$ ,  $\text{Cs}^{137}$ ,  $\text{Co}^{60}$  and ground radioactivity. The X-ray telescope had typical resolution of  $\sim 32\%$  at 59.6 keV ( $\text{Am}^{241}$ ). In Fig. 1, we have shown the detector response for  $\text{Am}^{241}$  and  $\text{Eu}^{152}$  and also the PHA linearity for this telescope. The typical resolution for gamma ray detection was 14.4% at 0.51 MeV ( $\text{Na}^{22}$ ). The anti-coincidence was adjusted at  $\sim 200$  keV monitoring the Compton response for  $\text{Cs}^{137}$  and  $\text{Co}^{60}$  sources. The rejection efficiency was adjusted at  $\sim 85\%$  for both the telescopes.

As the launch logistics at Commandante Ferraz base ( $58^{\circ}24'W$ ,  $62^{\circ}05'S$ ) favoured launches of small balloons, the payloads were covered with Styrofoam material for support and thermal insulation of the individual components of the telescope and no ballast or recovery system was attached. No onboard calibration and no graded shield for preventing X-rays entering from bottom side of crystal were provided for the X-ray telescope. The Raven balloon of  $\sim 7500\text{m}^3$  with the gamma ray payload ( $\sim 43\text{kg}$ ) was launched on the February 10, 1985 at 06:00 UT. The payload which was functioning until 15 minutes after launch ( $\sim 600\text{mbar}$  altitude) suddenly ceased transmission. The X-ray payload launched on February 21, 1985 at 06:30 UT, with a similar balloon attained a ceiling altitude of  $7,0\text{g}\cdot\text{cm}^{-2}$  after 100 minutes of ascent. The telemetry noise, especially frame synchronisation, permitted us to recover only 24 minutes of data at various altitudes of balloon ascent and 4 minutes of data at float altitude.

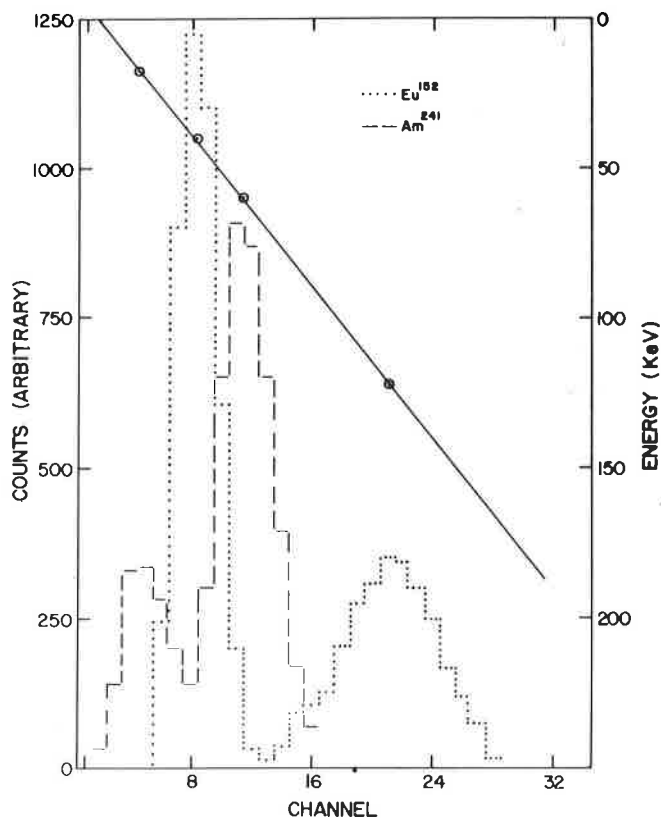


Figure 1 — The response of X-ray detector to  $\text{Eu}^{152}$  and  $\text{Am}^{241}$  radioactive sources. Also is shown the PHA energy calibration.

## RESULTS AND DISCUSSION

The premature termination of the gamma ray experiment flight permitted us to present the terrestrial activity obtained at Commandante Ferraz base in Antarctic and is shown in Fig. 2. The continuum spectrum, measured in the 200 keV to 2.9 MeV range, with the 7.62cm thick NaI(T1) crystal, exhibits power law indices and steep decline in flux beyond 2.8 MeV. The superposed peaks at 1.46 MeV ( $\text{K}^{40}$ ) and 2.6 MeV ( $\text{Th}^{228}$ ) are due to detector contamination and natural radioactivity. We have presented in the same figure the ground activity measured at Juazeiro do Norte ( $7^{\circ}3'S$ ,  $39^{\circ}12'W$ ) with a similar omnidirectional telescope consisting of a 10 x 10cm cylindrical NaI(T1) detector (Jayanthi et al. 1982). The flux in the continuum at the two places is essentially the same, since the 10 x 10cm crystal has higher efficiency of detection. However, it is clear from the total flux in the  $\text{Th}^{228}$  line, the radioactivity at Juazeiro do Norte is greater than that was measured at Commandante Ferraz base, at least factor  $\geq 2$ . The comparison in the radio activity of the two sites is not rigorous as we understand telluric activity measurements. However, it is an indication of the activity noticed by our detectors. This is expected as Juazeiro do Norte is situated in a known radioactive mineral region.

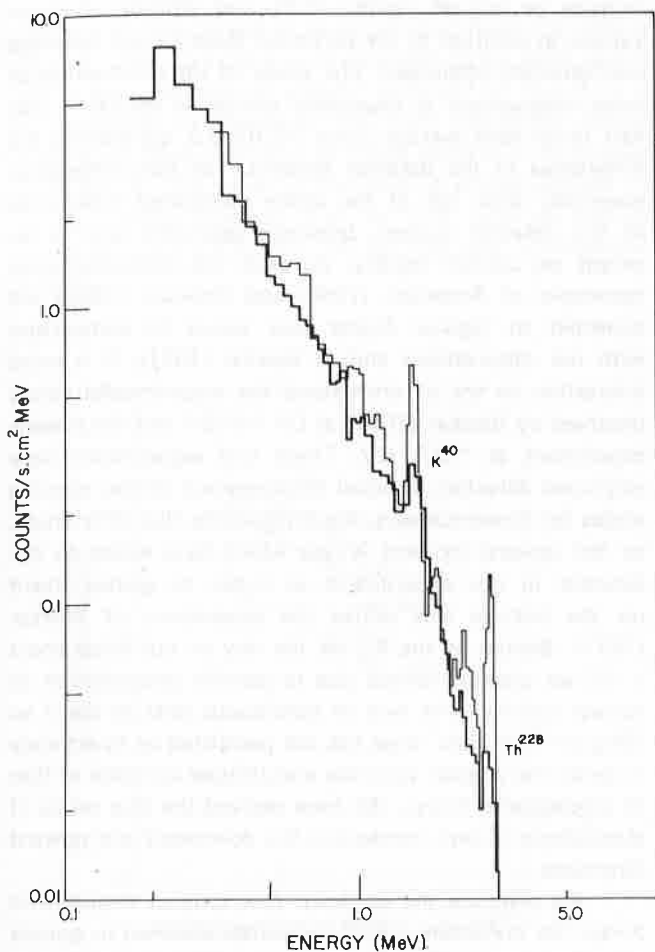


Figure 2 — The ground radioactivity histograms at Commandante Ferraz (thick line) and at Juazeiro do Norte (thin line) in gamma ray energy region.

The performance of the detector and associated electronics of the X-ray payload, were satisfactory during the ascent to the ceiling altitude of  $7.0g.cm^{-2}$ . However, the noise in the telemetry, permitted us to obtain useful data in two broad segments of altitude — 985 to 215 mbar and 22.2 to 6.85 mbar. In Fig. 3, the count rate time profile of the 28.5 to 100 keV and 100 to 180 keV X-rays is shown. We notice the characteristic fall in the count rate, in the initial phase, due to reduction in the terrestrial activity at the payload at 900 — 980 mbar altitude. As the balloon ascends further, the count rates show gradual increase and are expected to increase till Pfofzer maximum ( $\sim 120 - 150$  mbar). After this expected maximum, they decline to float altitude values as shown in the figure. As the cosmic ray secondaries cascade in the atmosphere the production rates of X-rays increase till Pfofzer maximum, as this altitude corresponds to mean free path length of the cosmic ray pion component.

The observed count rate spectra of the atmospheric X-rays at different altitudes are plotted in Fig. 4. The spectra at different depths have similar index of power law  $\sim 2.2$  in the energy range 50 to 150 keV and the flux values present the expected increase. The observed X-ray spectrum at ceiling altitude of  $\sim 7g.cm^{-2}$  is shown as a continuous histogram in Fig. 5. In the same figure, we have for comparison plotted the high altitude observations of Anderson (1960) at  $9.0g.cm^{-2}$ , Peterson (1963) at  $6.0g.cm^{-2}$  and Bleeker (1970) at  $4.3g.cm^{-2}$ .

The ceiling spectrum has been known to consist of three distinct components — the cosmic ray induced background (CRIB) in the detector, the atmospheric X-rays and cosmic X-rays. As discussed by Kasturirangan et al. (1971), the individual contributions of these components depend on the geomagnetic activity, geomagnetic

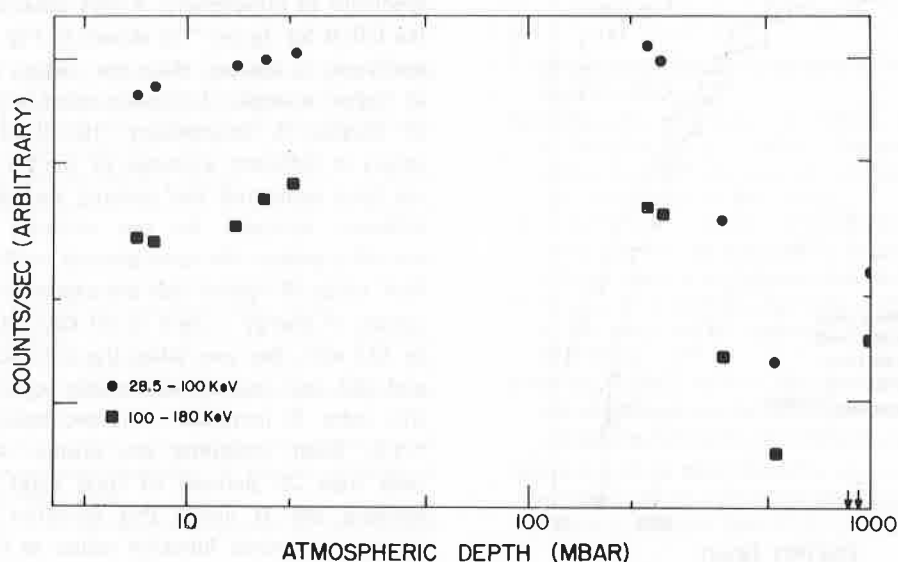


Figure 3 — Time history of X-ray count rate during the ascent of balloon to ceiling. Each observation corresponds to counts accumulated in 2 minutes time period in the energy band mentioned.

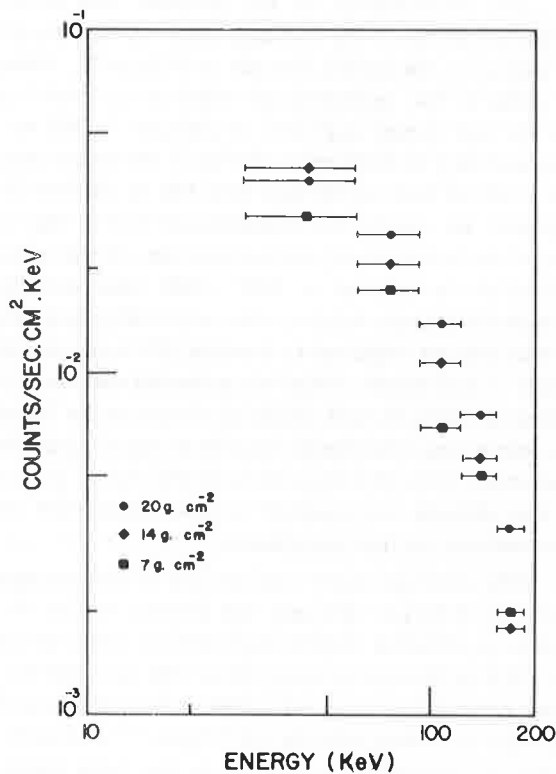


Figure 4 — The observed X-ray spectra at different altitudes.

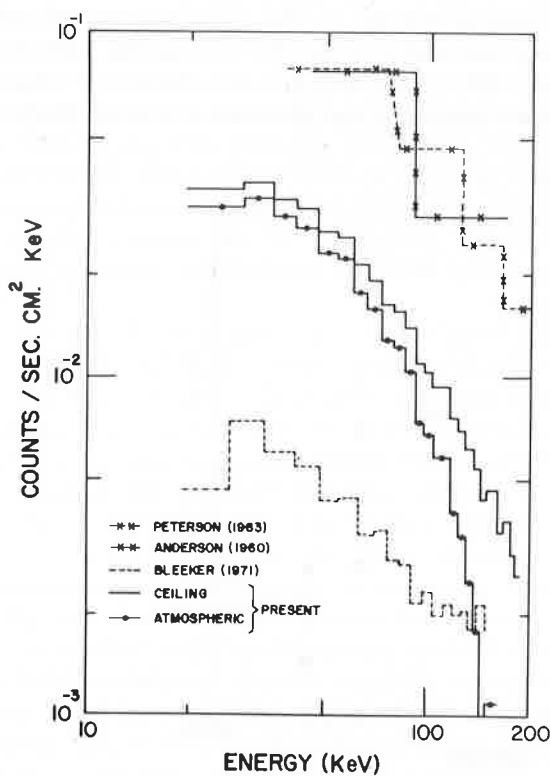


Figure 5 — The ceiling and atmospheric spectra observed in our experiment. High latitude ceiling spectra observed by other experimenters are also shown.

latitude or cut-off rigidity (CR) and altitude of observations in addition to the particular detector and telescope configuration employed. The shape of the spectrum in all these observations is essentially similar in the 50 – 150 keV range with average index  $\sim 2.0 \pm 0.2$ , considering the differences in the detector systems. The flux differences essentially arise out of the above mentioned differences of the detector system, telescope geometry and to an extent on cut-off rigidity. As such the omnidirectional telescopes of Anderson (1960) and Peterson (1963) are expected to register higher flux values in comparison with our observations and of Bleeker (1971). It is more interesting to try to understand the experimental values observed by Bleeker (1971) at CR  $\sim 5$  GV and the present experiment at  $\sim 3.1$  GV. These two experiments have employed detectors of equal thickness and similar opening angles for forward X-rays. We attribute the flux differences, to the upward incident X-rays which have access to the detector in our experiments as it has no graded shield on the bottom side unlike the experiment of Bleeker (1971). Besides as the  $K_p$  on the day of our experiment is  $\leq 2$  we discount excess due to particle precipitation or auroral activity. The lack of continuous data in the 7 to 200  $\text{g cm}^{-2}$  altitude range has not permitted us to estimate in detail the angular variation and altitude variation of flux of atmospheric X-rays. We have derived the flux ratios of atmospheric X-rays incident in the downward and upward directions.

We compare the up/down flux ratio of atmospheric X-rays for consistency with the values obtained in gamma ray range to justify the observed ceiling spectrum. We have estimated the contribution of cosmic ray induced background (CRIB) in our detector by interpolation to our cut-off rigidity and altitude values from the observations of Bleeker & Deerenberg (1970), who conducted identical experiments at three different latitudes. The spectrum of atmospheric X-rays obtained after subtracting the CRIB for  $7 \text{g cm}^{-2}$  is shown in Fig. 5. The atmospheric spectrum, is steeper than the ceiling spectrum especially at higher energies. In conjunction with the observations of Bleeker & Deerenberg (1970) of atmospheric flux values at different altitudes of the 25 to 110 keV X-rays, we have evaluated the upward and downward fluxes at different altitudes for our detector configuration and cut-off rigidity. We have plotted in Fig. 6, this up/down flux ratios  $R$  against the atmospheric depth for three intervals of energy – 28.5 to 60 keV, 60 to 92 keV and 92 to 123 keV. We have taken the statistics into consideration and did not include systematic errors. In all channels, this ratio  $R$  increases with decreasing depth by factors  $\sim 1.5$ . Even including the cosmic X-rays contribution (less than 20 percent of total flux) whose effect is to increase the  $R$  value, this variation with depth shows increase in source function values as in gamma rays. The decrease of values of up/down ratio with increase in energy is not expected. Perhaps, the fluorescent X-rays in lead and brass of the passive collimator, due to higher energetic X-rays in the up-ward direction, especially material nearer

the crystal contributed to more up-ward X-ray flux below 72 keV. This contribution is expected to be small and is difficult to estimate as angular variation of flux data is not available in literature. We treat the entire energy interval of 28 to 123 keV as single band with an average value for R. The value of the ratio at ceiling altitude of  $7\text{g}\cdot\text{cm}^{-2}$  varies between 2.57 to 1.55, with an average value of  $\sim 2.2 \pm 0.35$  for 28 to 123 keV atmospheric X-rays.

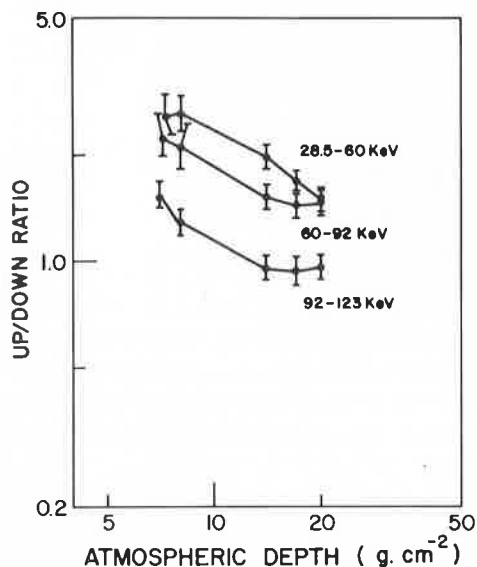


Figure 6 — Variation of the computed up/down atmospheric X-ray flux ratios with altitude and energy.

From the observations of gamma ray flux, in a  $7.62 \times 7.62\text{cm}$  NaI(Tl) detector, Ling (1975) evaluated the source functions and obtained for R values  $\sim 2.4$  and  $\sim 4.7$  at 300 keV and 1 MeV respectively for atmospheric gamma rays at  $7\text{g}\cdot\text{cm}^{-2}$  altitude. The experiment by Hsieh (1978) with a Compton telescope at 3.5 mbar float altitudes, has provided for the up/down flux ratios  $\sim 3.7$ , 3.85 and 5.6 at 2.5, 5.0 and 10.0 MeV respectively. The atmospheric build-up of flux due to the cascade interactions of cosmic ray secondaries, is expected to give lower values of R for X-ray region compared to gamma rays, as the latter have higher absorption mean free path length in the atmosphere. The up/down flux ratio value of R  $\sim 2.2$  for the 28 to 123 keV X-rays is not inconsistent with the higher gamma ray values. Thus we believe, the atmospheric spectrum observed in our experiment is due to cosmic ray secondary interactions in atmosphere with predominant contribution from upward incident X-rays.

#### ACKNOWLEDGMENTS

It gives us pleasure to acknowledge the constant support and encouragement of Prof. Pierre Kaufmann for these experiments. We thank Dr. N.A. BuiVan, J. Braga, C.D. Pritsopoulos, J.R. Chagas and N.B. Renó for their help in the design and fabrication of payloads and balloon launch operations. This work received financial support from CIRM-PROANTAR.

#### REFERENCES

- ANDERSON, K.A. — 1960 — Balloon observations of X-rays in the auroral zone. *J. Geophys. Res.*, **65**: 551-564.
- BLEEKER, J.A.M. — 1971 — The diffuse X-ray sky, PhD. Thesis, Leiden University, Leiden, 1971.
- BLEEKER, J.A.M. & DEERENBERG, A.J.M. — 1970 — The diffuse cosmic X-ray background from 20 to 200 keV. *Astrophys. J.*, **159**: 215-228.
- HSIEH, L.S. — 1978 — Atmospheric neutron and gamma ray fluxes and energy spectra at balloon altitudes. PhD. Thesis, University of New Hampshire, New Hampshire, 1978.
- JAYANTHI, U.B., BLANCO, F.G., AGUIAR, O.D., JARDIM, J.O.D., BENSON, J.L., MARTIN, I.M. & RAO, K.R. — 1982 — Spectral observations of atmospheric gamma ray background. *Rev. Bras. de Fís.* **12**: 431-442.
- KASTURIRANGAN, K. — 1971 — Secondary background properties of X-ray astronomical telescopes at balloon altitudes. *J. Geophys. Res.*, **76**: 3527-3533.
- LING, C.J. — 1975 — A semi-empirical model for atmospheric gamma rays from 0.3 to 10 MeV at  $\lambda = 40^\circ$ . *J. Geophys. Res.*, **80**: 3241-3252.
- MARTIN, I.M., RAI, D.B., DA COSTA, J.M., PALMEIRA, R.A.R. & TRIVEDI, N.B. — 1973 — Enhanced electron precipitation in Brazilian magnetic anomaly in association with sudden commencement. *Nature*, **240**: 84-86.
- PETERSON, L.E. — 1963 — The 0.5 MeV gamma ray and the low energy gamma ray spectrum to 6 grams per square centimeter over Minneapolis. *J. Geophys. Res.* **68**: 979-987.
- PINTO Jr., O. & GONZALEZ, W.D. — 1986 — X-ray measurements at the south Atlantic magnetic anomaly. *J. Geophys. Res.* **91**: 7072-7078.
- SEWARD, F.D. — 1973 — The geographical distribution of  $\sim 100$  keV electrons above the earth's atmosphere. Lawrence Livermore Laboratory, University of California, Livermore, (UCRL 51456).
- TEPLEY, L.R. & WENTWORTH, R.C. — 1962 — Hydromagnetic emissions, X-ray bursts and electron bunches — experimental results. *J. Geophys. Res.* **67**: 3317-3333.